

3D glass-ceramic scaffolds with antibacterial properties for bone grafting

Original

3D glass-ceramic scaffolds with antibacterial properties for bone grafting / VITALE BROVARONE, Chiara; Miola, Marta; Balagna, Cristina; Verne', Enrica. - In: CHEMICAL ENGINEERING JOURNAL. - ISSN 1385-8947. - 137:1(2008), pp. 129-136. [10.1016/j.cej.2007.07.083]

Availability:

This version is available at: 11583/1654565 since:

Publisher:

Published

DOI:10.1016/j.cej.2007.07.083

Terms of use:

This article is made available under terms and conditions as specified in the corresponding bibliographic description in the repository

Publisher copyright

(Article begins on next page)

3D-glass–ceramic scaffolds with antibacterial properties for bone grafting

C. Vitale-Brovarone *, M. Miola, C. Balagna, E. Vernè

*Politecnico di Torino, Materials Science and Chemical Engineering Department, Corso Duca degli
Abruzzi 24, 10128 Turin, Italy*

This is the author post-print version of an article published on *Chemical Engineering Journal*, Vol. 137, n. 1, pp. 129-136, 2008 (ISSN 1385-8947).

The final publication is available at:

<http://dx.doi.org/10.1016/j.cej.2007.07.083>

This version does not contain journal formatting and may contain minor changes with respect to the published edition.

The present version is accessible on PORTO, the Open Access Repository of the Politecnico of Torino, in compliance with the publisher's copyright policy.

Copyright owner: Elsevier.

* Corresponding author.

E-mail address: chiara.vitale@polito.it (C. Vitale-Brovarone).

Abstract

A 3D-scaffold for bone tissue engineering should show an interconnected macroporous network with pores exceeding 100 μm to favor cell penetration and vascularisation, should be osteoproliferative and should exhibit sufficient mechanical strength. In this work, bioactive glass ceramic scaffold characterised by a network of pores and struts were obtained using the sponge impregnation method. Specifically, 3D-scaffolds with a total porosity of 75 vol.% and 2MPa of compressive strength were prepared through a fine tuning of the processing parameters. On the as obtained scaffolds, silver ions were introduced in controlled amount through ion-exchange process imparting antibacterial properties.

Keywords: Glass–ceramic scaffold; Bone graft; Replication method; Antibacterial properties; Silver

1. Introduction

An optimal scaffold for bone tissue engineering should fulfill several criteria. First, the scaffold should be osteoconductive or even better osteoproliferative and it should serve as a 3D-template to provide structural support to the newly formed bone. For this purpose, it should consist of an interpenetrating network of pores and struts with open pores at least 100 μm wide to allow cell migration, tissue in-growth and vascularisation [1]. The scaffold should have mechanical properties matching that of the host bone and should bond to it without the formation of scar tissue, generating a stable interface. Crystalline ceramics such as hydroxyapatite, β -tricalcium phosphate and combinations of them have been widely studied as scaffolding materials [2–6] due to their similarity with the inorganic component of bone. More recently, glasses or glass–ceramics have been investigated as candidates for bone grafts as they are Class A bioactive materials which means they can bond to both bone and soft tissue and can stimulate bone growth [7]. The bond bonding ability of bioactive glasses is well known and has been ascribed to their capability of forming a surface layer of microcrystalline hydroxyapatite when put in contact with simulated body fluid [8]. More recently it has been discovered that the ionic dissolution products released from bioactive silica-based glasses up-regulate seven families of genes found in osteoblasts [9]. A number of techniques have been developed to fabricate porous glass–ceramic scaffolds, including starch consolidation, incorporation of volatile organic particles, foaming and replication of a polymeric sponge [10–14]. Specifically, the sponge method produces a highly open porous structure through the impregnation of a polyurethane sponge with a ceramic slurry of proper viscosity [14]. In order to maximize the

mechanical strength of the scaffold, different parameters such as solid loading of the ceramic slurry, type and amount of binder should be optimised. Moreover, the impregnation step and the removal of the exceeding slurry should be tuned in order to realise an adherent continuous coating of the polymeric skeleton with the glass particles, both at the sponge surface and within it. In such a way, after the sponge removal, a defect free 3D-scaffold with sufficient mechanical strength will be obtained. On the other hand, a well-known issue in surgery and in particular as far as orthopedic surgery is concerned, is the development of infections, due to bacterial colonisation of implanted materials. Though the discovery of antibiotics and the introduction of controlled hygienic protocols have remarkably minimised the risk of bacteria contamination during surgery and have decreased the danger of infection (2.5% in musculoskeletal surgery [15]), bacterial contagions can cause implant failure, prolong times and costs of hospitalisation, and sometimes lead to the patient's death [16,17]. Moreover in the last years, many nosocomial bacteria have shown an increasing selective resistance towards antibiotics, inhibiting the efficacy of preventive antibiotic prophylaxes [18]. For instance some micro-organisms are able to create a continuous slime, called biofilm, i.e. an extracellular polymer matrix consisting of glycoproteins and polysaccharides secreted by the bacteria themselves, that protects the micro-organisms; antibiotics are often unable to penetrate inside the biofilm and so bacteria adhered to the biomaterials surfaces can proliferate undisturbed. The first step of bacteria colonisation, the adhesion, is the most important event of biomaterials microbial infection and it is closely connected to surfaces nature; several surface treatments on biomaterials have been realised to decrease the risk of bacteria colonisation, in particular many antimicrobial agents have been used to modify the surface of biomaterials and obtain antibacterial properties. Silver is the most known antibacterial agent, it is used in different forms (ionic, metallic, colloidal, etc.) but, though the antibacterial activity of silver ions was demonstrated by several works [19–22], silver antimicrobial mechanism is not fully understood. It is well known that silver ions can interact with bacterial cells in different ways: they can bind to microbial DNA preventing bacteria replication or to sulfhydryl groups of bacteria enzymes, inhibiting cells respiration and bounding transport of important substances across the cells membrane and within the cells [23]. These different interaction ways are the origin of low silver bacteria resistance.

The aim of this work is to realise biocompatible, bioactive glass–ceramic scaffolds for bone grafts with antibacterial properties by introducing silver ions into the scaffolds surfaces through a patented ion-exchange process [24]. This technique allows, by tuning the process parameters, a controlled silver introduction in the superficial layers of the scaffold maintaining unchanged its structure and its characteristics. In such a way, an effective osteointegration due to the 3D-structure of the scaffold and of its bioactivity and bacteriostatic features can be obtained.

2. Materials and methods

A glass–ceramic containing fluoroapatite crystals with the following molar composition, 50% SiO₂, 18% CaO, 9% CaF₂, 7% Na₂O, 7% K₂O, 6% P₂O₅, 3% MgO (Fa-GC) was chosen to prepare the scaffold. Briefly, Fa-GC was prepared by melting the reactants in a platinum crucible at 1550 °C for 1 h and by quenching the melt in water to obtain a frit that was subsequently ball milled and sieved to a final grain size below 32 μm. Fa-GC molar composition was tailored by the authors in order to obtain a bioactive glass–ceramic containing fluoroapatite crystals and to propose it for bone substitutions and more specifically for dentistry applications. The differential thermal analysis (DTA- 7-Perkin Elmer) carried out on Fa-GC powders, showed a glass transition temperature ($T_g = 518$ °C), two crystallisation temperatures ($TX1 = 730$ °C, $TX2 = 780$ °C) and a softening range within 1200–1300 °C. X-ray diffraction (X'Pert Philips diffractometer) using the Bragg–Brentano camera geometry and the Cu K α incident radiation were carried out on quenched Fa-GC powders; the pattern analysis was carried out using X'Pert High Score software and the PCPDF data bank. The pattern of as poured Fa-GC showed the existence of an amorphous halo and of many diffraction peaks identified as fluoroapatite (PCPDF reference code 01-076- 0558). Hot stage microscopy was carried out on 3mm×3mm×3mm green compact cubes of Fa-GC to evaluate the volume modifications induced by crystallisation phenomena and shrinkages due softening, aiming to fix the thermal treatment for the scaffold production. To evaluate the bioactivity of Fa-GC, Fa-GC slices underwent a thermally treatment analogous to the one proposed for the scaffold (700 °C for 1 h) and were soaked in a simulated body fluid (SBF) for periods up to 1 month. Afterwards the samples were analysed by means of SEM observation and compositional analysis (EDS).

The technique chosen to realise the scaffold is the polymeric sponge method as reported in a previous paper for hydroxyapatite [3] and, by the authors, for a silica-based glass [14]. Briefly, a commercial polyurethane sponge, characterised by an open and interconnected macroporosity was cut in blocks of 1.5 cm×1.5 cm×1.5 cm or in bars of 1.5 cm×1.5 cm×5 cm and was impregnated with a slurry containing Fa-GC powders, polyvinyl alcohol as a binder and distilled water. The impregnated sponge was then compressed in an axial press to remove the exceeding slurry and afterwards it was dried at room temperature and then thermally treated to sinter the inorganic phase and to remove the organic skeleton. The impregnated sponge was thermally treated at 700 °C for 1 h; the sintering temperature was selected on the basis of hot stage microscopy in order to maximise the shrinkage and to allow a good sintering of Fa-GC particles. The microstructure of the obtained scaffolds was observed at scanning electron microscopy (SEM Philips 525M) to evaluate the degree of sintering, the pore interconnection and size, both on the scaffold surface and on its cross-sections.

The total pores content was evaluated by density measurements carried out on 10 specimens obtained from bars using the formula:

$$(1 - W_m/W_{th}) \times 100$$

where W_m is the measured weight and W_{th} is the theoretical one extracted from the product of glass density and the sample volume. To allow a fast cell migration inside the scaffold, the pore size and their degree of interconnection is a crucial feature and for this reason the porosity was further investigated on different scaffold cross-sections through image analysis (software Qwin Leica). This technique is useful to assess the pore size distribution and the total pore amount; it uses different SEM images on which a window size is selected and the porosity is highlighted by increasing the black and white contrast. Afterwards, the software elaborates the image as a binary picture identifying the dark area as pores: the equivalent pore diameter is then evaluated as $2(A/\pi)^{1/2}$ where A is the effective area calculated by the software. The acquired data can be further processed in order to plot them as bar charts reporting the pore numbers or the pore area versus the pore equivalent diameter. A capillarity test was carried out in order to evaluate the interconnection degree of the macro- and micropores; for this purpose a scaffold was put in contact with 5ml of a solution with a viscosity analogous to physiological fluids and obtained by mixing 30 wt.% of bovine serum and 70 wt.% of distilled water. Red ink drops were added to the prepared solution to better observe the capillary up-take of the fluid within the scaffold porosity. The degree of pores interconnection was evaluated on the basis of the adsorption rate of the solution; after the test the scaffolds were cut to verify the fluid up-take in its inner part. The mechanical strength of the scaffolds was evaluated by means of compressive test on different cubic samples (1 cm×1 cm×1 cm) using an Instron machine at a 1.0 mm/min crosshead speed; the compressive strength was calculated dividing the peak load for the resistant section. The mechanical characterisation was carried out on five specimens. On the as prepared scaffold, the ion-exchange technique [24] was applied soaking the scaffold in an aqueous silver nitrate solution in order to enrich the scaffold surface (its struts and the pore walls) with a controlled amount of Ag ions. The ion exchange process is a thermo-chemical treatment and involves the exchange of monovalent ions from the glass-ceramic with silver ions from the solution. Tuning the parameters that control the ion-exchange process (silver solution concentration, time and temperature of the process) is possible to modulate the amount of introduced silver ions and their concentration profile along the material section [19]. The process allows the silver introduction only in the superficial layers of the scaffold struts and of its pore walls without altering its bulk properties. Previous works have demonstrated that this technique permits the introduction of low and controlled silver amount without modifying

the Fa-GC characteristics and that the released silver is not cytotoxic [25]. In this research work, two different ion-exchange conditions have been chosen. Specifically, Ag-A-scaffold were obtained by dipping them in an aqueous silver nitrate solution (0.05 M) maintained at 100 °C for 45 min whereas Ag-B-scaffold were prepared by dipping them in the same solution at 37 °C for 8 h. The exchange conditions have been optimised on the basis of previous results obtained on various glass systems and on full density sintered Fa-GC [25], with the aim of introducing different amounts of Ag ions. The introduced silver amount was semi-quantitatively assessed through energy dispersion spectrometry (EDS Philips). The Ag content introduced inside Ag-A-scaffold was considered too high by the authors on the basis of previous works [19,20,25] and for this reason a more complete characterisation was carried out only on Ag-B-scaffold. The antibacterial properties were verified through the zone of inhibition test [26] using *Staphylococcus aureus* standard stock (ATCC 29213); the test was performed only on Ag-B-scaffold, on the basis of EDS semi-quantitative results. For this purpose, a bacterial broth has been prepared dissolving a *S. aureus* disk in 5ml of brain heart infusion; after overnight incubation at 37 °C, 10µl of the suspension have been spread on a Blood-Agar plate and incubated 24 h in order to allow the bacterial colonies to growth. Afterwards, a standard 0.5 Mc Farland (containing approximately $(1-2) \times 10^8$ CFU/ml) solution was prepared dissolving some bacterial colonies in a physiological solution (turbidity has been evaluated by optical instrument—Phoenix Spec BD McFarland) and then an aliquot of this suspension has been spread on Mueller Hinton agar plates. Afterwards Ag-B-scaffolds were incubated 24 h at 35 °C in the agar plate and the inhibition halo formation was observed and measured; the tests were done in triplicate.

3. Results and discussion

Fig. 1 reports a micrograph of a Fa-GC slice treated at 700 °C for 1 h and soaked in SBF for 2 weeks; as can be observed the surface is homogeneously covered by white globular shaped agglomerates rich in calcium and phosphorous with relative amounts analogous to hydroxyapatite. Fig. 2 reports a micrograph of the polymeric sponge used to obtain Fa-GC glass–ceramic scaffolds through the replication method. As can be observed, the polymeric template is characterised by an open macroporosity in the range of a few hundreds of µm highly interconnected with struts of a few tenths of µm. In the polymeric sponge method, the slurry tends to settle down at the bottom of the foam during the drying process which results in a nonhomogeneous porous structure after sintering. In order to avoid the Fa-GC particles settling, the polymeric template was impregnated with slurry of tailored characteristics containing 6 wt.% PVA, 35 wt.% of Fa-GC particles and the rest distilled water.

The slurry parameters were optimised thorough the evaluation of impregnated sponge at SEM (data non-reported) obtained with amount of Fa-GC powders within 25 and 35 wt.% and PVA content within 2 and 6 wt.%. The slurry obtained with 25 wt.% Fa-GC particles led to sponges not perfectly impregnated with quite a few polymeric struts not covered by Fa-GC particles. When the content of the binder was increased from 2 wt.% till 6 wt.%, a better covering of the polymeric skeleton was achieved. In fact, by increasing the binder content, the Fa-GC particles are more uniformly covered by PVA enhancing their ability to stick together onto the polymeric struts. For the template impregnation, the sponge was soaked three times in the Fa-GC suspension and each time it underwent a removal phase of the exceeding slurry by compressing the impregnated sponge up to 60% in order to avoid clogged pores formation.

Based on hot stage microscopy results, in order to take advantage of Fa-GC shrinkage maximising the degree of sintering and the scaffold mechanical strength, the impregnated sponge was thermally treated at 700 °C for 1 h. The proposed thermal treatment induced the complete burnout of the polymeric template and the sintering of Fa-GC particles obtaining 3D-scaffolds. The obtained scaffolds showed a white colour due to a complete removal of both the sponge and PVA in accordance with thermogravimetric analysis results of the sponge that showed its complete elimination just below 600 °C. It is known that pyrolysis of the polymeric template is crucial in sintering ceramics with the polymer sponge method [27] and for this reason the burnt out of the sponge should be completed before the Fa-GC particles begin to soften. In this study, heating rate of 5°/min till 700 °C with a dwell time of 1 h was successfully used to obtain the scaffolds. The proposed treatment led to a glass–ceramic structure with a not negligible residual amorphous phase as can be observed in Fig. 3. At this purpose, Fig. 3 reports the diffraction patterns of as poured Fa-GC powders (a) and of the obtained scaffold after grinding (b) in order to compare them. The analysis of the diffraction pattern of the scaffold leads to the identification of fluoroapatite (JCDD 01-076-0558) and of a second phase identified as canasite (JCDD 00-013-0553). The presence of canasite in the glass–ceramic is a positive attribute as this phase is highly biocompatible and has been proposed for glass–ceramic for hard-tissue augmentation [28]. The texture due to the glass–ceramic nature of the obtained scaffold is a positive feature as it enhances the surface area and cell adhesion and proliferation [2]. The shrinkages values due to Fa-GC softening and sintering were evaluated on five different scaffolds shaped as bars; the scaffolds were measured after the thermal treatment and showed the following shrinkages: linear $25\pm0.6\%$ and volumetric $62\pm2\%$. The obtained shrinkage values are characterized by a very low standard deviation indicating a good reproducibility of the proposed process. Besides, a controllable volumetric shrinkage would allow obtaining scaffolds of precise size and profile by carefully shaping the polymeric template. For this

reason, the sponge impregnation method represents a valid processing technique as allows producing scaffolds with irregular shapes to match that of the defect in the bone of the patient. The scaffolds were observed at SEM to evaluate the porosity distribution and the pore dimension; Fig. 4a and b shows the morphology of the scaffold surface and of its cross-section, respectively. A scaffold for bone graft should act as a template for tissue growth in three-dimensions and should have an interconnected macroporous network containing pores with diameters exceeding 100 μm [29]. SEM images in Fig. 4 show a continuous 3D-interpenetrating network of struts and pores very similar to cancellous bone. As it can be observed in Fig. 4 most of the pores are open and a few hundred μm wide in good accordance with the optimum pore size reported by Hubert et al. [30] Fig. 5a shows a magnification of the scaffold in which two pores can be better observed as well as the scaffold structure underlying them. The observed pore size and interconnecting porous structure are suitable for cell penetration and migration, tissue in-growth and vascularisation and nutrient supply within the bone graft [1,7,31]. Fig. 5b depicts a magnification of the pores trabeculae in which the high degree of sintering is observable; the original Fa-GC particles cannot be individuated due to a complete densification process. The good sintering level showed that the choice of the thermal treatment was successful both for the effective removal of the polymeric template and for the densification of the pores struts. The glass–ceramic nature of the obtained scaffold can be seen in Fig. 5b where a lot of crystals under a continuous amorphous layer can be observed in good accordance with the XRD pattern obtained for the scaffold and reported in Fig. 3. The well sintered and continuous struts are very positive features of the scaffold as they are essential for maximizing the scaffold mechanical strength. The compression strength, evaluated by means of a compression test on five cubic samples were $2\pm0.6\text{MPa}$ which is considered a good value for bone grafts as reported by many authors. The compression tests showed that all samples exhibit a linear elastic region followed by a collapse plateau dominated by brittle fracture of the scaffold struts in accordance to the data reported by Ramay for hydroxyapatite scaffold [3]. The density measurement showed an average porosity of $74.6\pm3.4\%$: this is a very encouraging result because an elevated degree of porosity is necessary to allow a fast vascularization of the bone graft. The density data were corroborated by the image analysis results; Fig. 6a reports the analysed area of the scaffold and Fig. 6b and c shows the bar charts relatives to the pores area distribution along the scaffold surface and its cross-section. As can be observed, most of the pore area is occupied by large voids which are useful for cell migration and tissue in-growth. Fig. 7a and b reports in a bar chart the number of micropores below 50 μm and macropores above 50 μm both on the scaffold surface and on its cross-section: as can be observed all along the scaffold a high number of micropores is present, above 50% of the total pore number. The presence of small pores on the scaffolds struts is

due to the removal of the polymeric skeleton and is constant all along the scaffold section. Microporosity is a crucial feature because it results in large surface area that is believed to contribute to protein and cell adhesion; moreover the glass–ceramic nature of the obtained scaffold results in a high roughness which enhances attachment and proliferation of bone forming cells [2,32]. The mechanical strength of a porous material depends on the density of the pores struts as suggested by Gibson and Ashby [33]. On the other hand a high porosity provides a favorable biological environment and maximize the scaffold ability of being rapidly vascularised: a balance between the porosity and the density of the scaffold should be achieved. The obtained scaffolds have porosity around 75 vol.% and a mechanical strength of 2MPa and thus represent a good balance for bone grafts if compared to other data reported in the literature and in the ISO standard [13,34,35].

The capillarity test carried out on a 1 cm³ cubic scaffold showed an up-take time of 2 s during which the whole scaffold became red due to the presence of ink drops in the simulated blood fluid as can be observed in Fig. 8a. After up-taking the scaffold was cut in two pieces in order to better observe its cross-section which was completely coloured in red as shown in Fig. 8b. The high ability of Fa-GC scaffolds of being rapidly and uniformly impregnated by simulated blood and its aptitude of retaining the up-taken fluid are due to the presence of macropores and above all by an interconnected network of micropores that rapidly adsorbed the fluid by capillarity. At this purpose, Fig. 9 reports a SEM magnification of a pore and of its trabeculae containing a lot of micropores due to the pyrolysis of the polyurethane foam. The presence of this residual microporosity is a positive feature as it promotes proteins and cells adhesion onto the scaffold struts without lowering too much the mechanical strength. The as prepared scaffolds were doped with silver with ion-exchange technique in aqueous solution as reported by Di Nunzio and Vernè [24]. Two different conditions were tested in order to load different amount of silver ions: Ag-A-scaffold and Ag-B-scaffold will indicate the samples obtained using the higher and the lower temperature of exchange, respectively. Fig. 10a and b reports the EDS results on the analysis carried out on the scaffolds surface after the ion-exchange phase using conditions A and B, respectively. A much higher silver amount was exchanged using condition A (about 15 wt.%) whereas a remarkably lower silver content was observed for Ag-B samples (about 5 wt.%). These results are in good accordance with previous studies carried out on bulk glasses by the authors [19] in which a too high silver content was found to affect cells vitality [20]; for this reason it was chosen to focus future characterisation only on Ag-Bscaffolds. The zone of inhibition test clearly discloses an antibacterial behaviour of Ag-B-scaffolds; all tested samples are able to create an inhibition halo of about 2–3mm showing the effectiveness of the ion-exchange process to induce a bacteriostatic behavior towards *S. aureus*

stock. Fig. 11 shows a Mueller Hinton agar plate containing three Ag-B-scaffolds and one untreated scaffold as a control; bacteria are inhibited to grow all around the three silver treated samples, instead they proliferate close the untreated one. The inhibition zone is a qualitative test that demonstrates the bacteriostatic behaviour of introduced silver amount: silver-doped scaffolds are able to inhibit the bacteria proliferation, but it is impossible with this test to be sure of their ability of killing bacteria colonies. Further tests are in progress in order to deeply investigate the antibacterial behaviour of the produced scaffolds and their biocompatibility.

4. Conclusions

The use of the polymeric sponge method was successful in obtaining a 3D-interpenetrating network of pores and struts similar to trabecular bone. The scaffold is characterised by open macropores larger than 100 μm and thus suitable for bone in-growth, cell penetration and vascularisation. A good balance within porosity and mechanical strength was attained with 75 vol.% of pores and 2MPa of compressive strength. The presence of a diffused microporosity on the scaffold struts was observed and will favor, along with the glass–ceramic texture, proteins and cell adhesion onto the 3D-scaffold enhancing the biological response. Moreover, the used glass–ceramic composition (Fa-GC) will favor the scaffold osteointegration due to its bioactivity. The ion-exchange process was successfully applied on the prepared scaffold and an antibacterial effect was observed through the formation of an inhibition halo for the silver loaded scaffold; additional work is in progress in order to further investigate the scaffold antibacterial properties and their biocompatibility.

Acknowledgements

The authors wish to thank Dr. S. Di Nunzio, Ing. S. Ferraris (DISMIC Polito) and Dr. G. Fucale (CTO) for their helpful discussion and assistance during antibacterial tests. This research was partially funded by “Funzionalizzazione di materiali vetrosi ad azione antibatterica per dispositivi di osteosintesi” granted by Regione Piemonte (2004) and by EU Network of Excellence project Knowledge-based Multicomponent Materials for Durable and Safe Performance (KMM-NoE) under the contract no. NMP3-CT-2004-502243.

References

- [1] M. Freyman, I.V. Yannas, L.J. Gibson, *Prog. Mater. Sci.* 46 (2001) 273–282.
- [2] V. Karageorgiou, D. Kaplan, *Biomaterials* 26 (2006) 5474–5491.
- [3] H. Ramay, M. Zhang, *Biomaterials* 24 (2003) 3293–3302.
- [4] J. Dong, H. Kojima, T. Uemura, M. Kikuchi, T. Tateishi, J. Tanaka, *J. Biomed. Mater. Res.* 57 (2) (2001) 208–216.
- [5] H. Yuan, K. Kurashina, J.D. de Beuijn, Y. Li, K. De Groot, X. Zhang, *Biomaterials* 20 (19) (1999) 1799–1806.
- [6] C. Zhang, J. Wang, H. Feng, B. Lu, Z. Song, X. Zhang, *J. Biomed. Mater. Res.* 54 (3) (2001) 407–411.
- [7] L.L. Hench, J.M. Polak, *Science* 295 (2002) 1014–1017.
- [8] L.L. Hench, *J. Am. Ceram. Soc.* 81 (1998) 1705–1728.
- [9] I.D. Xynos, A.J. Edgar, L.D.K. Buttery, L.L. Hench, *J. Biomed. Mater. Res.* 55 (2001) 151–157.
- [10] C. Vitale-Brovarone, S. Di Nunzio, O. Bretcanu, E. Vernè, *J. Mater. Sci.: Mater. Med.* 15 (2004) 209–217.
- [11] C. Vitale-Brovarone, E. Vernè, P. Appendino, *J. Mater. Sci.: Mater. Med.* 17 (2006) 1069–1078.
- [12] T. Livingston, P. Ducheyne, J. Garino, *J. Biomed. Mater. Res.* 62 (2002) 1–13.
- [13] J. Jones, L. Ehrenfried, L.L. Hench, *Biomaterials* 27 (2006) 964–973.
- [14] C. Vitale-Brovarone, E. Vernè, L. Robiglio, P. Appendino, F. Bassi, G. Martinasso, G. Muzio, R. Canuto, *Acta Biomater.* 2 (2007) 199–208.
- [15] L. Rimondini, M. Fini, R. Giardino, *J. Appl. Biomater. Biomech.* 31 (2005) 1–10.
- [16] M. Confalonieri, E. Damonti, *GIMMOC VII* 1 (2003) 21–26.
- [17] D. Campoccia, L. Montanaro, C.R. Arciola, *Biomaterials* 27 (2006) 2331–2339.
- [18] A. Kumar, P.H. Schweizer, *Adv. Drug Deliv. Rev.* 57 (2005) 1486–1513.
- [19] S. Di Nunzio, C. Vitale Brovarone, S. Spriano, D. Milanese, E. Vernè, V. Bergo, G. Maina, P. Spinelli, *J. Eur. Ceram. Soc.* 24 (2004) 2935–2942.
- [20] E. Vernè, S. Di Nunzio, M. Bosetti, P. Appendino, C. Vitale-Brovarone, G. Maina, M. Cannas, *Biomaterials* 26 (2005) 5111–5119.
- [21] M. Kawashita, S. Tsuneyama, F. Miyaji, T. Kokubo, H. Kozuka, K. Yamamoto, *Biomaterials* 21 (2000) 393–398.
- [22] J.J. Blaker, S.N. Nazhat, A.R. Boccaccini, *Biomaterials* 25 (2004) 1319–1329.

- [23] W. Chen, Y. Liu, H.S. Courtney, M. Bettenga, C.M. Agrawal, J.D. Bumgardner, J.L. Ong, *Biomaterials* 27 (2006) 5512–5517.
- [24] S. Di Nunzio, E. Vernè, Process for the production of silver-containing prosthetic devices. PCT/EP2005/056391.
- [25] E. Vernè, S. Ferraris, M. Miola, S. Di Nunzio, R. Canuto, G. Muzio, G. Maina, Fucale, C. Vitale-Brovarone, *J. Mater. Sci. Mater. Med.*, submitted for publication.
- [26] NCCLS M2-A9 Performance Standards for Antimicrobial Disk Susceptibility Tests, Approved Standard, Ninth Edition.
- [27] H.S. Li, J.R. De Wijn, P. Layrolle, K. de Groot, *J. Biomed. Mater. Res.* 61 (2002) 109–120.
- [28] J.R. Jones, L.L. Hench, *Curr. Opin. Solid State Mater. Sci.* 7 (2003) 301–307.
- [29] N. Kancharanat, C. Miller, P. Hatton, P. James, I. Reaney, *J. Am. Ceram. Soc.* 88 (2005) 3198–3204.
- [30] S.F. Hubert, J.S. Morrison, J.J. Klawitter, *J. Biomed. Mater. Res.* 6 (1972) 347–374.
- [31] N. Okii, S. Nishimura, K. Kurisu, Y. Takeshima, T. Uozumi, *Neurol. Med. Chir.* 41 (2001) 100–104.
- [32] L.L. Hench, *Curr. Opin. Solid State Mater.* 2 (1997) 604–610.
- [33] L.J. Gibson, M.F. Ashby, *Cambridge Solid State Science Series*, 2nd ed., Cambridge University Press, Cambridge, UK, 1997, pp. 429–452.
- [34] I. Jun, Y.H. Koh, H.E. Kim, *J. Am. Ceram. Soc.* 89 (1) (2006) 391–394.
- [35] Implants for surgery-hydroxyapatite. Part1. Ceramic hydroxyapatite BS ISO 13779-1:2000.

FIGURES

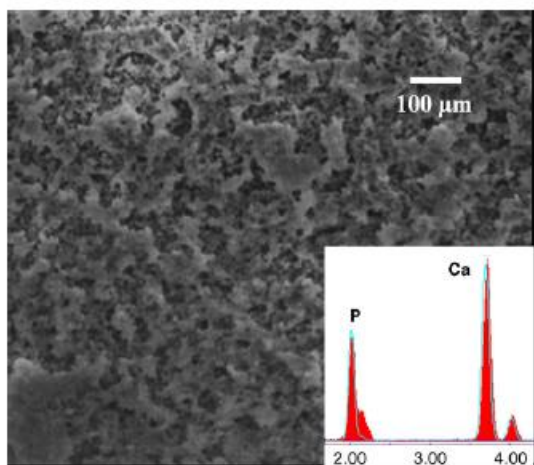


Fig.1 SEM micrograph and EDS analysis of the Fa-GC surface after 2 weeks in SBF

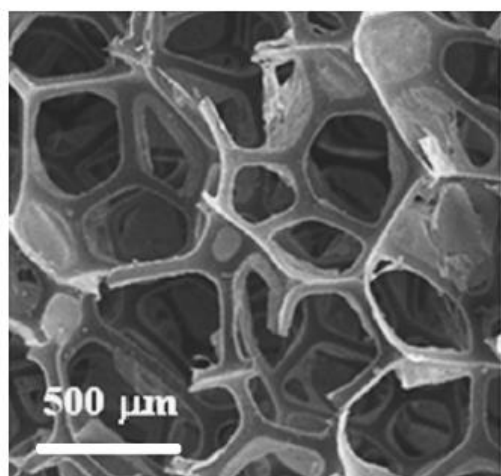


Fig.2. SEM micrograph of the polymeric template

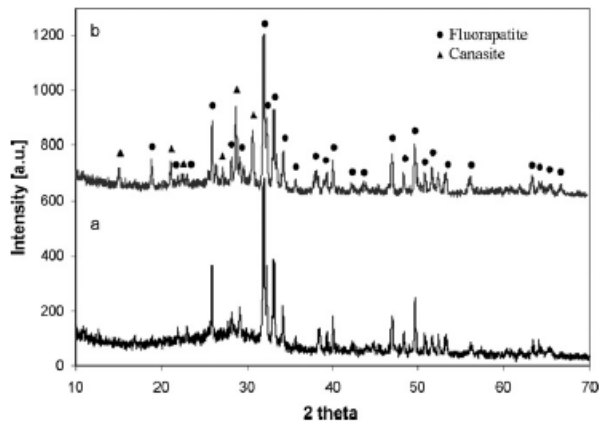


Fig.3. Diffraction patterns of as poured Fa-GC (a) and of the scaffold (b)

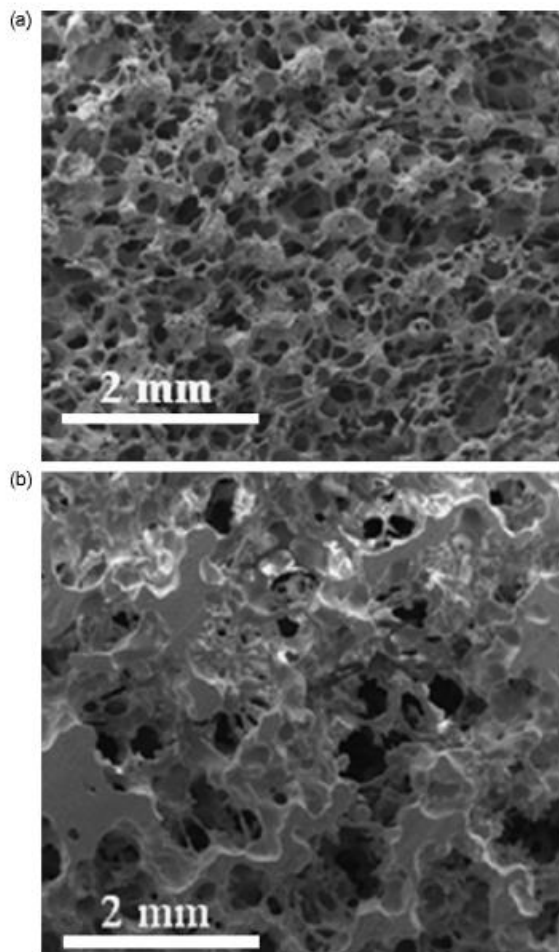


Fig.4. SEM micrographs of the scaffold surface (a) and of its cross-section (b)

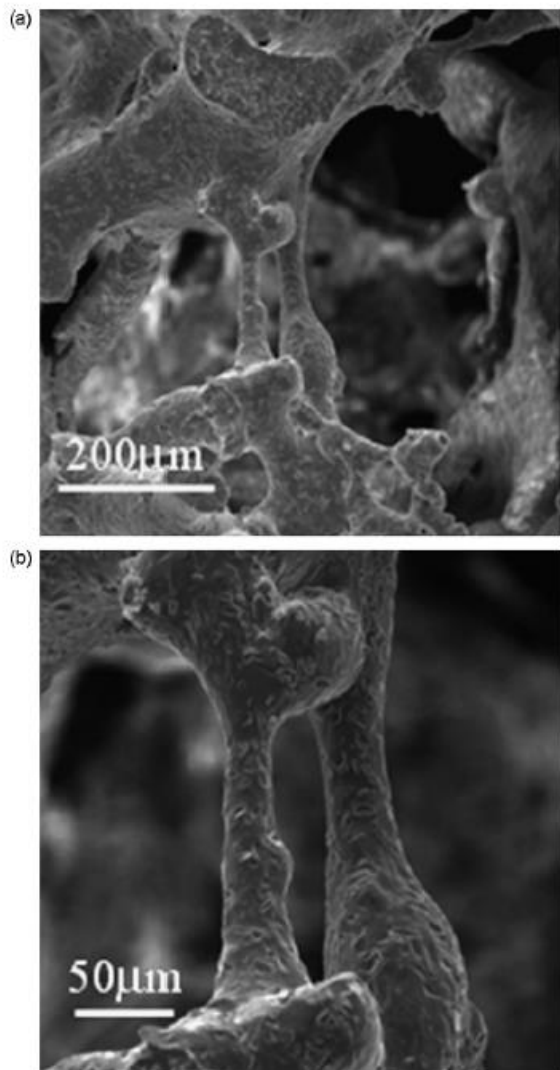


Fig. 5. SEM micrographs of macropores at different magnifications

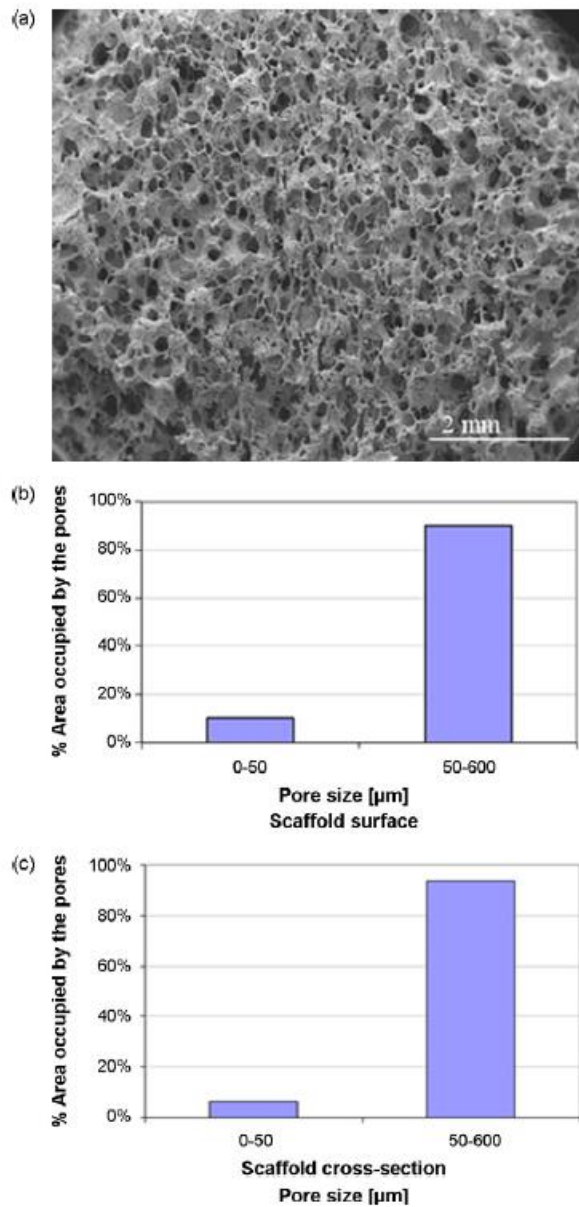


Fig.6. Selected area for the image analysis (a), bar chart of the area occupied by the pores on the scaffold surface (b) and on its cross-section (c)

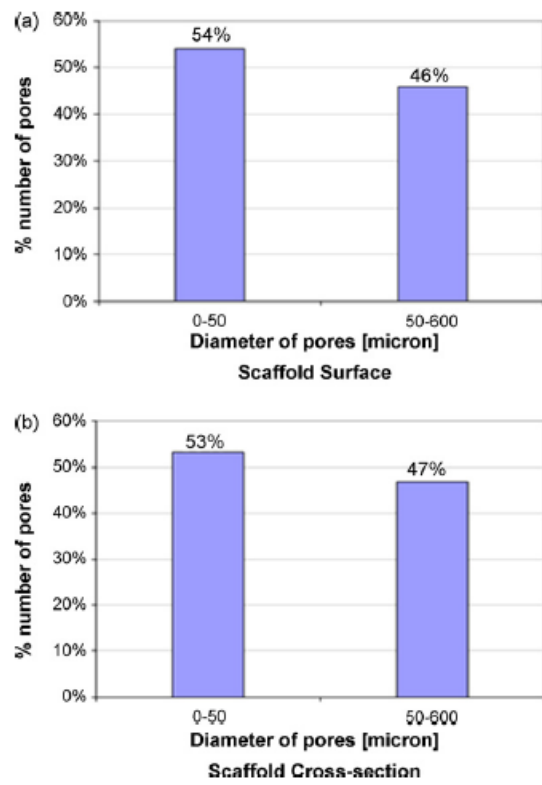


Fig.7. Bar chart of the pore numbers on the scaffold surface (a) and on its cross-section (b)

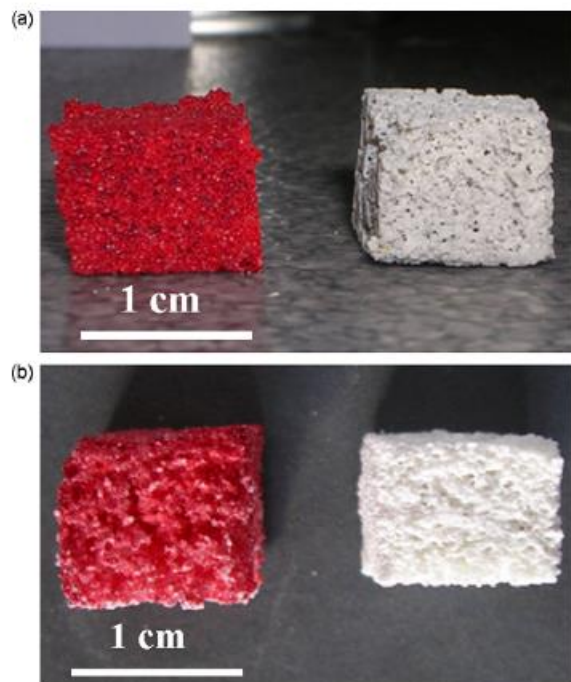


Fig. 8. Images of the scaffold before and after capillarity test: scaffold (a) and cross-section (b)

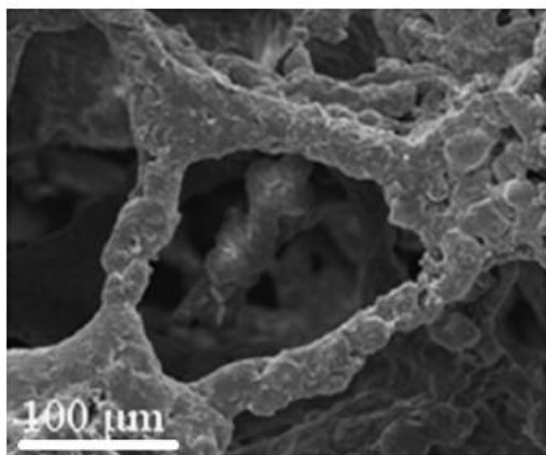


Fig. 9. SEM micrograph of a pore and its struts

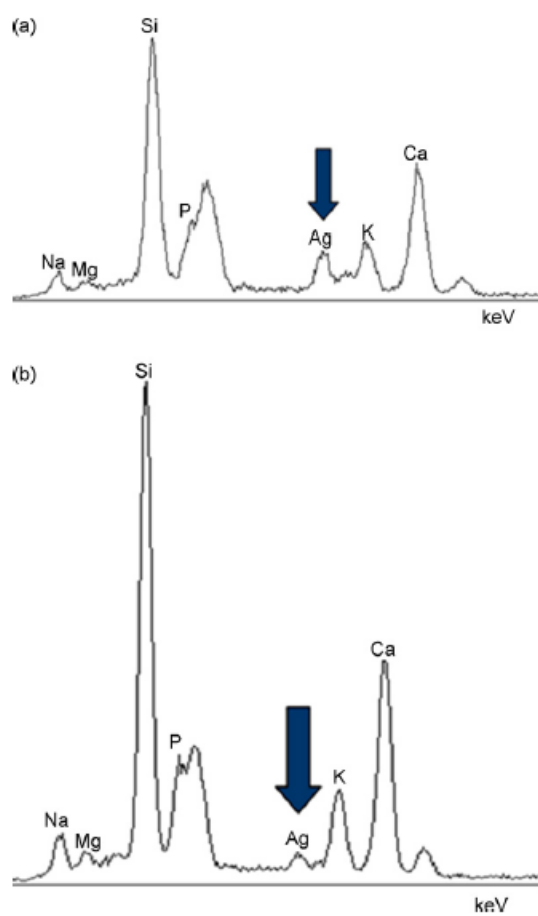


Fig. 10. EDS analyses on Ag-A-scaffold and Ag-B-scaffold surfaces

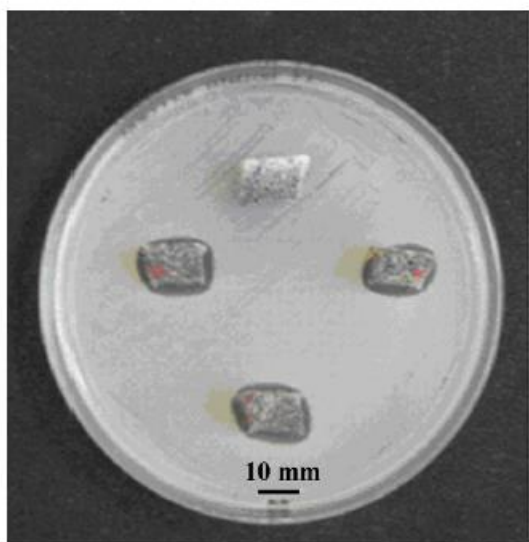


Fig.11. Inhibition zone test for the Fa-GC scaffold and for three Ag-B-scaffolds